Scientific Research Publishing

Advances in Bioscience and Biotechnology, 2024, 15, 269-288
https://www.scirp.org/journal/abb
ISSN Online: 2156-8502
ISSN Print: 2156-8456

HISP-1 Inhibits HSV-1 Infection in Cultured Vero Cells

Sandra D. Adams[1*], Kevin T. Bilyk[1], Modukuri V. Ramani[2], Gottumukkala V. Subbaraju[2]

[1]Department of Biology, Montclair State University, Montclair, USA
[2]Department of Chemistry, Andhara University, Visakhapatnam, India
Email: *adamssa@montclair.edu

How to cite this paper: Adams, S.D., Bilyk, K.T., Ramani, M.V. and Subbaraju, G.V. (2024) HISP-1 Inhibits HSV-1 Infection in Cultured Vero Cells. *Advances in Bioscience and Biotechnology*, **15**, 269-288.
https://doi.org/10.4236/abb.2024.154017

Received: January 20, 2024
Accepted: April 27, 2024
Published: April 30, 2024

Abstract

Herpes simplex virus-1 (HSV-1) remains a leading cause of viral disease worldwide and is spread by direct contact with infected lesions. There is no vaccine against HSV-1 infections and there remains a need to identify therapeutics that could reduce the spread. In this study various hispolon compounds were analyzed to determine their antiviral potential against HSV-1 infections in cultured Vero cells. To determine the effects on infectivity and possible mechanisms of inhibition, the following assays were conducted. *In vitro* cytotoxicity assays were conducted to determine the effect of the compounds on cell viability and the maximum non-cytotoxic concentrations. Antiviral assays measured cell viability, percent inhibition of infection following treatment with the compounds, and the effect on the viral infection cycle. These effects were visualized using inverted light and fluorescent microscopy. Of the 24 hispolons tested, only hispolon pyrazole-1 (HISP-1) demonstrated antiviral effects. HISP-1 was demonstrated to effect early stages in HSV-1 infection in cultured Vero cells (attachment, penetration, and post-penetration). In silico modeling analyses were conducted to analyze the interactions between HISP-1 and viral glycoprotein D (gD). HISP-1 is safe at concentrations tested and is effective in inhibiting infection of HSV-1 in cultured cells. HISP-1 has potential for therapeutic use as an antiviral against HSV-1 infection, could work in synergy with other antivirals that work be a different modality, and could be developed as a component of a topical agent to reduce the spread of HSV-1 infections.

Keywords

Hispolon, Herpes Simplex Virus-1, Antiviral, Curcumin

1. Introduction

Hispolon (HIS) is a polyphenolic bioactive compound isolated from the fruiting

body and mycelium of medicinal mushroom *Phellinus linteus*. HIS demonstrated a range of medicinal properties including antioxidant, anti-inflammatory, and antiproliferative effects [1] [2] [3] [4]. Additionally, hispolon ethanolic extracts from the fruit bodies of the basidiomycete *Inonotus hispidus* reported antiviral activity against influenza types A and B [5]. Curcumin, a natural phenolic compound derived from *Curcuma longa*, has demonstrated a broad therapeutic potential including antioxidant [6], anti-inflammatory [7] [8], antibacterial [9], and antiviral activities against hepatitis C virus [10], enterovirus 71 [11], human immunodeficiency virus [12], influenza A [13], and herpes simplex virus (HSV) 1 and 2 [14] [15]. Curcumin is mostly insoluble in water, poorly soluble in hydrocarbon solvents, but very soluble in polar solvents such as ethanol, methanol, and dimethyl sulfoxide (DMSO) [16]. Low bioavailability has been attributed to curcumin being insoluble in water at pH 7 [17]. The poor bioavailability of curcumin reduces its potential as a therapeutic agent with clinical applications [18].

The World Health Organization estimates that 67% of the world's population over the age of 50 is infected with HSV-1 [19]. HSV is transmitted by close contact [19]. HSV receptor-binding protein, glycoprotein D (gD) is the principal determinant for viral entry [20]. The herpesvirus entry pathway requires the coordinated action of gD, gH/L heterodimer and gB. Glycoprotein B is a class III fusogenic protein essential for HSV-1 infectivity, thought to undergo a conformational change that provides energy for membrane fusion [21]. The use of antiviral agents such as acyclovir and ganciclovir can lead to resistance [22] and there still is no effective vaccine against HSV infections. Since the virus can enter a latent stage and can develop resistance to antivirals, it is important to continue to search for novel antiviral agents.

There are structural similarities between hispolon and curcumin [23]. Analogues of curcumin and structurally related hispolon analogues were developed to compare their effectiveness as anti-inflammatory and anti-proliferative agents against various cancers [24]. Additionally, 44 hispolon compounds were synthesized and screened for antitubercular and antibacterial activity [25]. X-ray crystal structures and computational docking techniques were used to compare the antiproliferative activity of hispolon and several derivatives to curcumin [26]. This study aimed to compare the antiviral properties of various hispolon compounds against HSV-1.

2. Materials and Methods

2.1. Cell Culture

Vero cells (American Type Culture Collection (ATCC) Manassas, VA) were cultured in T25 flasks using Dulbecco's Modified Eagle Medium (DMEM) media supplemented with 5% Fetal Bovine Serum (FBS) (Serum Source International, Charlotte, NC, USA) and 1% gentamicin sulfate (BioWhittaker, Lonza, VWR, South Plainfield, NJ, USA). Trypsin EDTA (0.25%) was used to subculture cells. The cells were maintained at 37˚C and 5% CO_2.

2.2. Preparation of Virus

A recombinant strain of HSV-1, GHSV-UL46 (ATCC VR-1544), which contains the sequence for green fluorescent protein (GFP) fused to the tegument protein pUL46 [27] was used for all experiments. Virus was passaged in T25 flasks and Vero cells were allowed to display full cytopathic effect (CPE). The media containing virus was then collected, centrifuged, and the supernatant stored at −80˚C.

2.3. Preparation of Hispolons

Twenty-four compounds [Hispolon (HIS) 1-6, hispolon isoxazoles (HISI) 1-6, hispolon phenylsulpho pyrazoles (HISPSP) 1-6), and hispolon pyrazoles (1-6)] (Natsol Laboratories Pvt. Ltd., Visakhapatnam, India) were dissolved in DMSO to prepare 5 mM stock solutions. Hispolon concentrations were then diluted in DMEM to desired concentrations of 12.5, 25, 50, 75, 100, and 125 μM.

2.4. Cytotoxicity Study—Alterations of Cell Morphology

Vero cells were plated in 6 well plates, grown for 24 hours and treated with various concentrations (12.5, 25, 50, 75, 100, and 125 μM) of each of the 24 hispolon compounds. After 1 hour (h) the hispolon reagents were removed by aspiration and the cells were washed with phosphate buffered saline (PBS). DMEM was then added to the wells and cells were incubated at 37˚ under 5% CO_2 and observed every 24 hours for a period of three days after treatment. Cells were examined, using an inverted microscope, at 400× magnification to observe morphological changes in the cells.

2.5. Antiviral Assays—Inverted Microscopic Observation

Cell treated assay—Vero cell suspensions (100 μL) were plated in separate wells in a 6 well plate and after 24 - 48 hours (when 70% - 80% confluent) cells were treated with various concentrations of hispolons (12.5, 25, 50, 75, 100, and 125 μM) for 60 minutes, then aspirated. Cells were infected with 100 μL of HSV-1. After 1 hour, all unadsorbed virus was aspirated and replaced with 3 mL DMEM. After 48 hours, infected cells were examined with an inverted microscope at 400× magnification to observe cytopathic effect in the cells.

Virus treated assay—Vero cell suspensions (100 μL) were plated in separate wells in a 6 well plate for 24 hours. HSV-1 virions were treated with various concentrations of hispolons (12.5, 25, 50, 75, 100, and 125 μM) for 60 minutes. After 60 minutes, Vero cells were infected with treated virus for 1 hour. After 1 hour, all unadsorbed virus was aspirated and replaced with 3 mL of media. After 48 hours, infected cells were examined with an inverted microscope at 400× magnification to observe cytopathic effect in the cells.

2.6. Antiviral Assays—Cell Proliferation

2.6.1. Cell—Treated Assay

Vero cell suspensions (100 μL) were plated in separate wells in a 96 well plate and after 48 hours cells were treated with various concentrations of hispolons

(25, 50, 75, and 100 μM) for 60 minutes, then aspirated. Cells were infected with 100 μL of HSV-1. After 1 hour, all unadsorbed virus was aspirated and replaced with 100 μL of DMEM. After 48 hours, 20 μL of MTS reagent was then added to the samples; the plate was gently rocked, then incubated at 37˚C under 5% CO_2 for 60 minutes. The absorbance was measured at 450 nm using Infinite PRO 200 microplate reader (Tecan Life Sciences US, Raleigh, NC USA).

2.6.2. Virus—Treated Assay

Vero cell suspensions (100 μL) were plated in separate wells in a 96 well plate for 48 hours. HSV-1 virions were treated with various concentrations of hispolons (25, 50, 75, and 100 μM) for 60 minutes. After 60 minutes, Vero cells were infected with treated virus for 1 hour. After 1 hour, all unadsorbed virus was aspirated and replaced with 100 μL of media. After 48 hours, 20 μL of MTS reagent was then added to the samples; the plate was gently rocked, then incubated at 37˚C under 5% CO_2 for 60 minutes. The absorbance was measured at 450 nm using Infinite PRO 200 microplate reader (Tecan Life Sciences US, Raleigh, NC USA).

$$\%\ \text{Viability} = \left[\left(\text{Cells infected with treated HSV-1} - \text{Blank}\right)/\left(\text{Cells only} - \text{Blank}\right)\right] \times 100.$$

2.7. Binding Assay

Vero cells were grown for 24 - 48 hours in a 96-well plate until 70% - 80% confluent. The plate was pre-incubated at 4˚C for 30 min. Subsequently, the media was removed from the cells. The virus was treated with increasing concentrations (25, 50, 75, and 100 μM) of HISP-1 Treated and untreated HSV-1 virions were incubated at room temperature for 1 h followed by infection of the cells on ice. The plate was incubated for 1 h at 4˚C, then unbound HSV-1 was carefully aspirated from the cells using a multichannel pipettor.

Fresh media was added to cells in each well. The plate was incubated at 37˚C and 5% CO_2 for 48 h and assayed using the Viral ToxGlo™ assay (Promega, Madison, WI, USA) as described previously. Mean and SD (four replicates) were calculated using Graph Pad Prism (GraphPad Software, Inc., La Jolla, CA).

2.8. Penetration and Post-Penetration Assays

Vero cells were grown in a 96-well plate until 70% - 80% confluent. The media was removed from the cells and the cells were infected with 100 μL of HSV-1. The plate was incubated at 4˚C for 2 h to ensure attachment but not penetration of the HSV-1. At room temperature various concentrations (25 - 100 μM) of HISP-1 were added. The plate was incubated at room temperature for 10 min for the penetration assay. For the post-penetration assay, various concentrations (25 - 100 μM) of HISP-1 were added for 30 min at room temperature after the virus particles entered the cells. After incubation, 100 μL of 1× phosphate buffer saline (PBS) (pH 3.0) was added to each well to inactivate the unadsorbed virions for 1 minute immediately followed by addition of 100 μL of 1× PBS (pH 11.0) to neutralize the acid. The PBS and media were removed using a multichannel pipettor

followed by the addition of 100 µL of 5% FBS DMEM. After 48 h, cell viability was determined using the Viral ToxGlo™ (Promega, Madison, WI, USA) assay. The plate was read using the Infinite 2000 PRO microplate reader (Tecan Life Sciences US, Raleigh, NC USA). Mean and SD (five replicates) were calculated using Graph Pad Prism (GraphPad Software, Inc., La Jolla, CA).

2.9. Fluorescent Microscopy

Vero cells were grown on glass cover slips in 6-well plates and incubated at 37˚C and 5% CO_2 until 70% - 80% confluent. When confluent, the cells were infected with HSV-1 treated with 75 µM HISP-1 or untreated HSV-1 for 1 h. Uninfected cells served as a negative control. Cells infected with untreated virus served as positive control. After one hour of infection the unadsorbed virions and media were aspirated from the cells and replaced with media. Twelve hours post infection, the cells were treated with 300 µL of DAPI (4,6-diamidino-2-phenylindole) (Sigma Aldrich) stain for 5 min at 37˚C in the dark. Then the cells were fixed with 2% - 4% paraformaldehyde for 10 - 20 min then rinsed with PBS. Mounting medium, containing 90% glycerol, and 10% phosphate buffered saline (PBS) was used to fix the coverslips on the slides. Slides were permanently sealed around the perimeter using clear nail polish. The slides were observed using a Zeiss Axio Scope A1 microscope (Zeiss US, Peabody, MA, USA).

2.10. Molecular Docking Analyses

The crystallized structure for the receptor, glycoprotein D (4MYV), was obtained from the Protein Data Bank (https://doi.org/10.2210/pdb4MYV/pdb). Non-standard residues were then removed in UCSF Chimera [28] and the receptor was prepared for docking in UCSF Chimera and Auto Dock Tools [29]. The grid space for docking was then defined for this protein in Auto Dock Tools based on insight from CastP [30] analysis of glycoprotein D binding pockets.

A 3D model for hispolon pyrazole 1 ((E)-4-(2-(3-Methyl-1H-pyrazol-5-yl) vinyl) benzene-1,2-Diol) was not available; this was created by first creating the chemical structure in Biovia Draw Version 22.1 (2022). This structure was imported into ChemSketch (ChemSketch, version 2022.1.2) where this was converted into a 3D structure; this structure was then refined using Avogadro [31]. Finally, this molecule was prepared for docking using Auto Dock Tools. The 3D structure for Curcumin was downloaded from PubChem (https://pubchem.ncbi.nlm.nih.gov/compound/Curcumin, accessed on 1/4/2024) which was then prepared for docking in Auto Dock Tools.

The docking analysis was carried out using Auto Dock Vina [32] [33] to test for an interaction between either of the target ligands (hispolon pyrazole 1 or curcumin) and glycoprotein D. A binding affinity of −7.0 kcal/mol was used as a threshold to identify significant interactions. Results were visualized in Auto-DockTools to review binding affinity, then in Biovia Discovery Studio Version 24.1.0.23298 (2023) to generate figures.

2.11. Statistical Analyses

All statistical analyses were performed on raw absorbance or luminescence values and are presented as means ± standard error of the mean (SEM). Data were analyzed separately using a one-way ANOVA with treatment as the main variable in GraphPad Prism (GraphPad Software, Inc., La Jolla, CA). The source of significant main effects was queried using post hoc analysis, and significant interactions were assessed with pairwise comparisons. For all test results, a predetermined level of $\alpha = 0.05$ was used.

3. Results

3.1. Treatment with Hispolon Compounds Is Not Cytotoxic to Vero Cells

Cytotoxicity to each of the hispolon compounds was assayed at a concentration range of (12.5 -125 μM). The effect of 2% concentration of DMSO was also assayed since the hispolons were dissolved in DMSO. Microscopic analyses indicated that the Vero cells were not affected by the DMSO vehicle even when cells were treated with concentrations up to 2.5% DMSO. These results are consistent with the findings of a previous study [34]. There were no morphological changes in cells following treatment with each of the hispolon compounds up to the tested concentration of 125 μM (**Figure 1**).

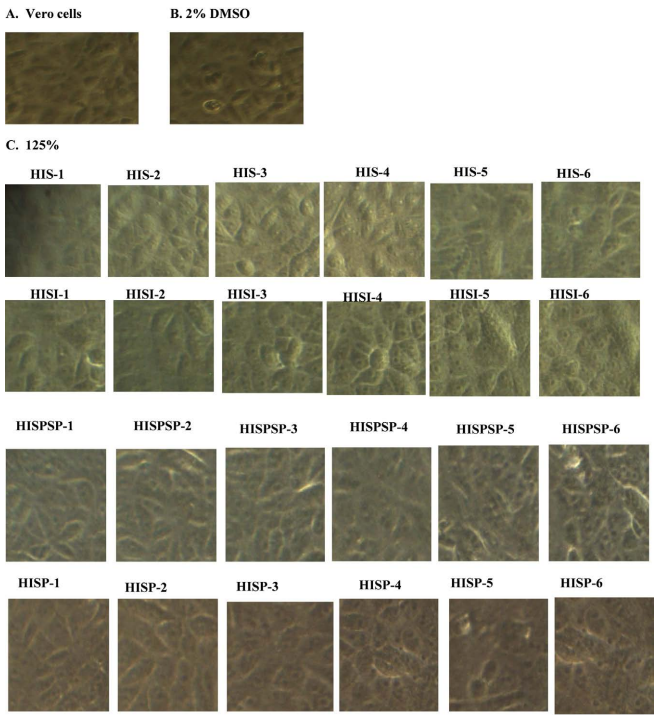

Figure 1. Microscopic observation (400×) of cell morphology under different conditions (A) Control, Vero cells only; (B) Vero cells treated with 2% DMSO; (C) Vero cells treated with the maximum concentration (125 μM) of each hispolon compound. The results indicate that the DMSO and hispolons are not cytotoxic to Vero cells at concentrations tested.

3.2. Treatment with HISP-1 Inhibits Infection in Vero Cells

3.2.1. Inverted Microscopic Study

Vero cells infected with HSV-1 display cytopathic effects. The microscopic assay was designed to determine which of the hispolon compounds could inhibit HSV-1 infection of cultured Vero cells. In the cell-treated assay, Vero cells were treated with various concentrations (12.5 - 125 μM) of each of the hispolon compounds. Treated cells were then infected with HSV-1. In the virus-treated assays, HSV-1 virions were treated with each of the hispolon compounds at various concentrations (12.5 - 125 μM). Treated virions were then used to infect Vero cell monolayers. Infected cells were observed for evidence of CPE and microscopic images were taken at 48 hours post infection (hpi). Of the 24 hispolon compounds tested, only HISP-1 (Figure 2) reduced the appearance of CPE and increased cell viability (Table 1, Figure 3). Reduction in the appearance of CPE indicated that treatment with HISP-1 inhibited HSV-1 infection of cultured Vero cells. Microscopic examination indicated that treatment with HISP-1 reduces or prevents HSV-1 induced cytopathic effects.

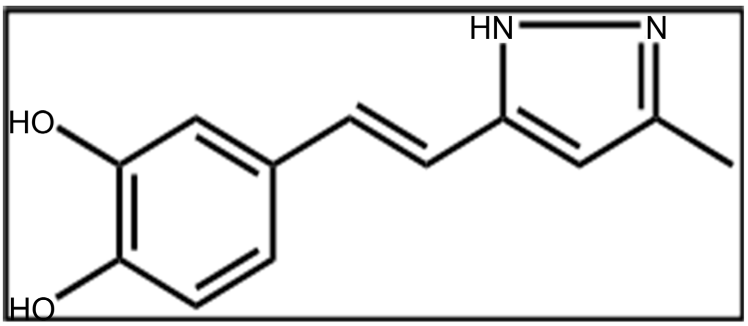

HISP-1: $C_{12}H_{12}N_2O_2$

Figure 2. Chemical and structural formulas for HISP-1.

Table 1. Only HISP-1 reduced the appearance of cytopathic effects of HSV-1 infections of Vero cells at concentrations ranging from 50 - 125 μM.

HISPOLON (HIS) Inhibition?	Hispolon isoxazoles (HISI) Inhibition?	Hispolon phenylsulpho pyrazoles (HISPSP) Inhibition?	Hispolon pyrazoles (HISP) Inhibition?
HIS-1—No	HISI-1—No	HISPS-1—No	HISP-1 (50 - 125 μM)
HIS-2—No	HISI-2—No	HISPS-2—No	HISP-2—No
HIS-3—No	HISI-3—No	HISPS-3—No	HISP-3—No
HIS-4—No	HISI-4—No	HISPS-4—No	HISP-4—No
HIS-5—No	HISI-5—No	HISPS-5—No	HISP-5—No
HIS-6—No	HISI-6—No	HISPS-6—No	HISP-6—No

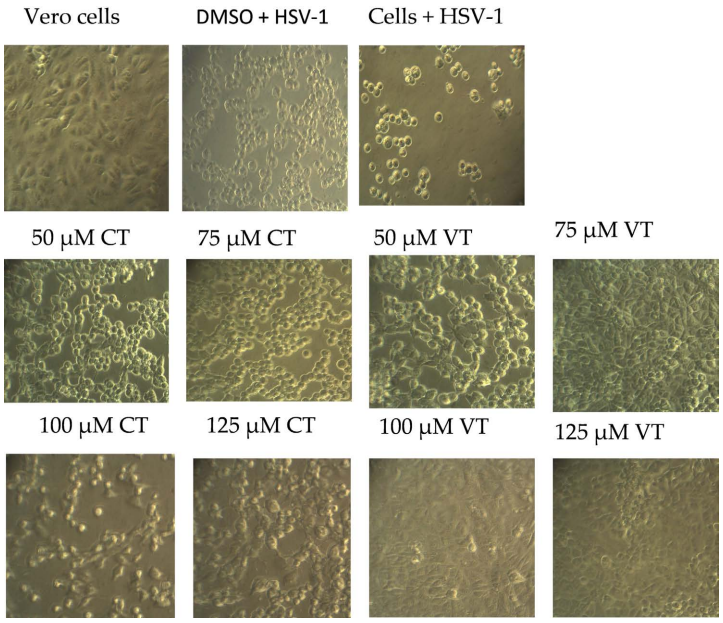

Figure 3. Inverted microscopic observations (400×) of Vero cells, Vero cells treated with DMSO and infected with HSV-1, and untreated HSV-1 infected controls; cells treated with 50, 75, 100 and 125 μM concentrations of HISP-1 then infected with HSV-1 (CT-cell treated), and virions treated with 50, 75, 100 and 125 μM concentrations of HISP-1that were used to infect Vero cell monolayers. Rounded and lifted Vero cells indicate CPE.

Infection of Vero cells with HSV-1 treated with HISP-1 at concentrations ranging from 75 - 125 μM did not indicate evidence of CPE. Monolayers are intact with no appearance of rounding and lifting, like the Vero cells control. There was evidence of cytopathic effect when cells were treated prior to infection (CT) with HSV-1 and when virions were treated with less than or equal to 50 μM concentration of HISP-1. Cells treated with 2% DMSO prior to infection with HSV-1 also showed evidence of CPE (**Figure 3**).

3.2.2. Treatment with HISP-1 Increased Cell Proliferation

The ability of HISP-1 to mediate HSV-1 induced cell damage was investigated by determining the effect on cell viability. Cell viability of Vero cells infected with HSV-1 following treatment of Vero cells with 50 - 125 μM (CT) or treatment of HSV-1 virions (VT) with HISP-1 was determined using an MTS assay, which quantifies viable cells using the insoluble formazan product as an indicator of cell proliferation. The mean value of percent viability of Vero cells infected with HSV-1 treated with 50, 75, or 100 μM HISP-1 was significantly greater as compared to the mean value of percent viability of Vero cells infected with untreated HSV-1. For HISP-1 treated HSV-1 at 75 and 100 μM concentrations, the percentages of viable cells are 78.8 and 78.4, respectively. Treatment of cells before infection with concentrations up to 125 μM of HISP-1, however, was not significantly different from the percent of viable cells resulting from infection with untreated virus (**Figure 4(A)**). The percent inhibition of infection also differed significantly when HSV-1 was treated with concentrations of 50, 75, or 100 μM

HISP-1 as compared to infection of Vero cells with untreated HSV-1. The greatest percentage of inhibition was observed with the 75 μM and 100 μM HISP-1 treated HSV-1 with percentage of inhibition 62.7 and 63.1, respectively. Percent inhibition, as measured by the MTS assay is shown in Figure 4(B).

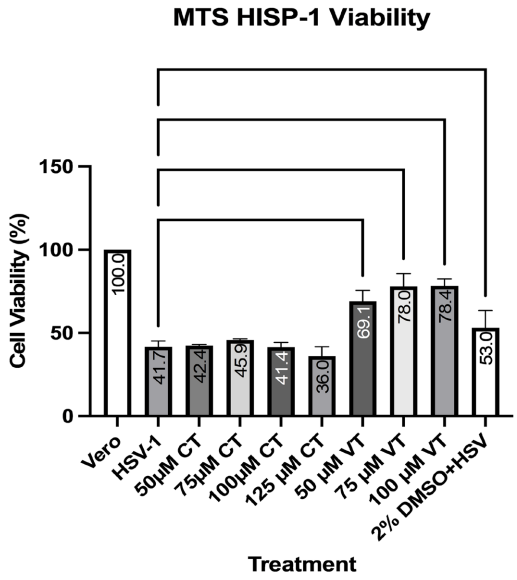

(A)

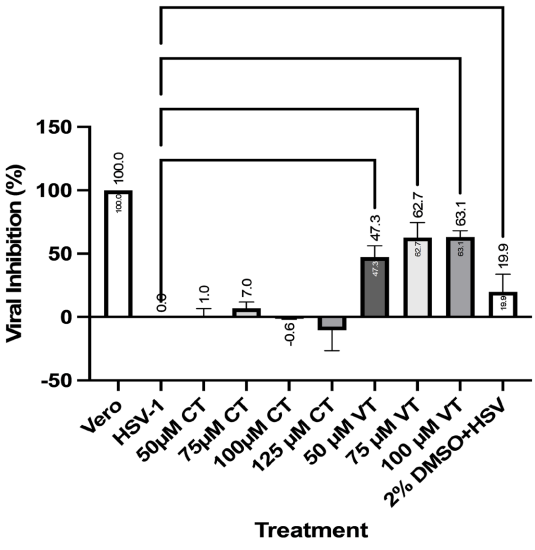

(B)

Figure 4. Treatment of HSV-1 virions affects cell proliferation of HSV-1 infected cells. HSV-1 mediated cell death was significantly inhibited in Vero cells following treatment of the virions with HISP-1. Cell viability of Vero cells (5 replicates) (CT) or Vero cells (5 replicates) (VT) was quantified 48 hpi using the Cell-Titer 96Aqueous One Solution Cell Proliferation Assay (MTS) (Promega). Vero cells infected with treated HSV-1 had higher viability compared to untreated infected cells after 48 h (A). The % inhibition calculated based on these viabilities was significantly different when cells were infected with HISP-1 treated virus (B). Data are presented as mean ± SEM. Statistical analysis was performed for the viability assay using a one-way ANOVA with Tukey's HSD Test for multiple comparisons comparing results to the untreated HISP-1 infected control, *$p < 0.5$, ****$p < 0.0001$.

3.2.3. Treatment of HSV-1 Virions with HISP-1 Increased Cell Viability

An additional measure of cell viability was used to assess the effect of treatment with HISP-1 with a maximum concentration of 75 μM. The goal was to determine the lowest concentration of the compound that would inhibit HSV-1 infection. The Viral ToxGlo™ Assay measures ATP levels as an indicator of mitochondrial function and cell viability. Cell viability was measured by luminescence. HISP-1 treatment increased ATP production in infected Vero cells. Treatment of Vero cells (cell treated indicated by CT) and HSV-1 virions with HISP-1 resulted in significant differences in cell viability as compared to percent viable cells when infected with untreated HSV-1. The greatest percentage of viable cells (70.6%) was observed when the virus was treated with 75 μM HISP-1 (**Figure 5(A)**). The percent inhibition of infection also differed significantly when HSV-1 was treated with concentrations of 25, 50, or 75 μM HISP-1 as compared to infection of Vero cells with untreated HSV-1. The greatest percentage of inhibition (56.8%) was observed with the 75 μM HISP-1 treated HSV-1 (**Figure 5(B)**).

3.3. HISP-1 Affects Early Stages of the Infection Process of HSV-1

The antiviral activity of HISP-1 on the binding to host cells was assessed using a binding assay. Vero cells were infected with HSV-1 treated with increasing concentrations of HISP-1 for 1 h at 4˚C. This allowed for the binding to occur but not the penetration of the virus [35]. After 48 h, luminescence was measured. There were significant differences between the attachment or binding of treated virions and untreated virions (**Figure 6(A)**). The difference in the effect on binding, as measured by luminescence, was significant when antiviral activity was calculated following treatment of HSV-1 with 50, 75, and 100 μM concentrations of HISP-1 with greatest calculated value for attachment occurring with 75 μM concentration (**Figure 6(A)**). This indicates that HISP-1 inhibits the binding stage of the HSV‐1 infection cycle.

To determine the antiviral effects of HISP-1 during penetration of the virus into the host cell, Vero cells grown in a 96 well plate were infected with HSV‐1 at 4˚C for 2 h to ensure attachment but not penetration of the virions. The cells were treated for 10 min at varying concentrations (25 μM to 100 μM) of HISP-1 at room temperature during the penetration step [35] of infection. After 48 h, luminescence was measured. There were significant differences between the penetration of treated virions and untreated virions. The greatest effect was seen when Vero cells were infected with virions treated with 75 μM HISP-1. This indicates that HISP-1 inhibits the penetration stage of the infection cycle.

The antiviral effect of HISP-1 on the post penetration step of the viral cycle was determined by infecting Vero cells with HSV-1 at 4˚C for 2 h to ensure attachment but not penetration of the HSV-1. Cells were then treated with HISP-1 for 30 min at 37˚C and 5% CO_2 after the virus penetrated the cells. Cell viability was measured 48 hpi. The results indicated that treatment with HISP-1 after

binding and penetration did affect HSV-1 infection. There was a significant difference in viable cells resulting from treatment post-penetration of virions treated with 75 μM HISP-1 as compared to untreated virions. Treatment of virions with HISP-1 inhibits binding, penetration and post penetration stages of the HSV-1 infection cycle.

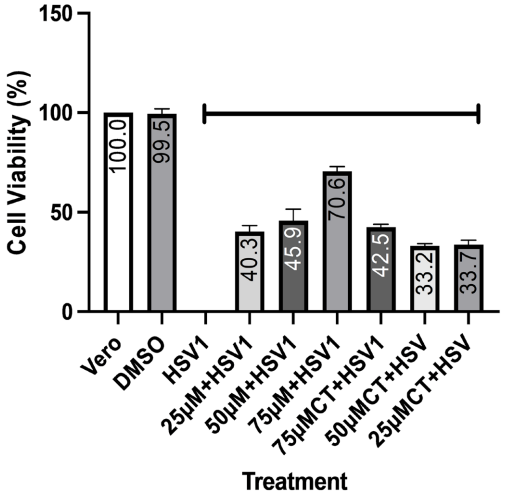

(A) ToxGlo Viability

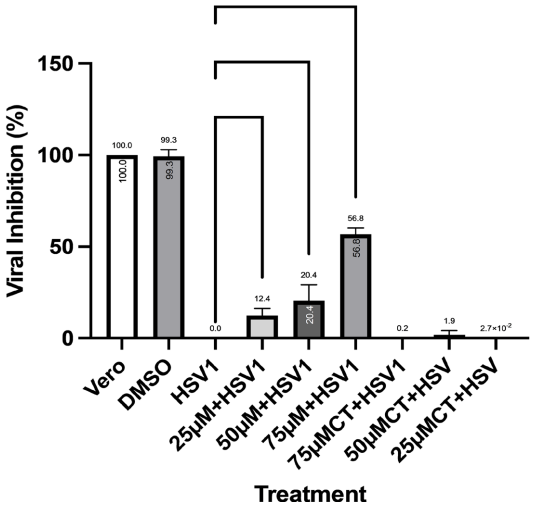

(B) ToxGlo Inhibition

Figure 5. Treatment with HISP-1 affects cell viability of HSV-1 infected cells. HSV-1 mediated cell death was significantly inhibited in Vero cells following treatment of the cells or treatment of the virions with HISP-1. Cell viability of Vero cells (5 replicates) was quantified 48 hpi using Viral ToxGlo™ assay kit (Promega Corp., Madison, WI*)* (Promega). There was a significant difference in percent viability of cells treated (CT) with HISP-1 or when virions were treated with HISP-1 when compared to infection with untreated HSV-1 (A). The % inhibition calculated based on these viabilities was significantly different when cells were infected with HISP-1 treated virus and compared to infection of Vero cells with untreated HSV-1 (B). Data are presented as mean ± SD. Statistical analysis was performed for the viability assay using a one-way ANOVA with Tukey's HSD Test for multiple comparisons comparing results to the untreated HISP-1 infected control, *$p < 0.5$, ***$p < 0.001$, ****$p < 0.0001$.

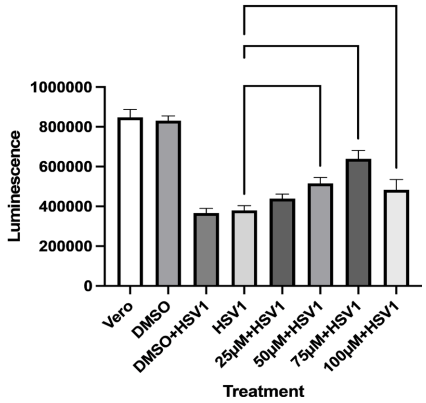

(A) Binding

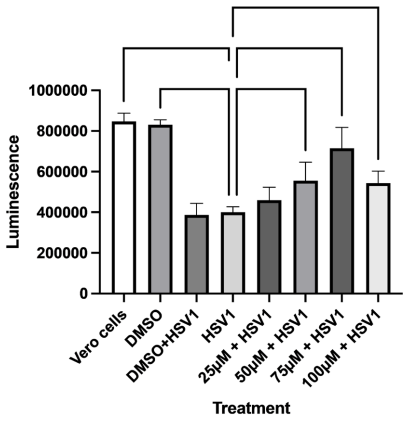

(B) Penetration

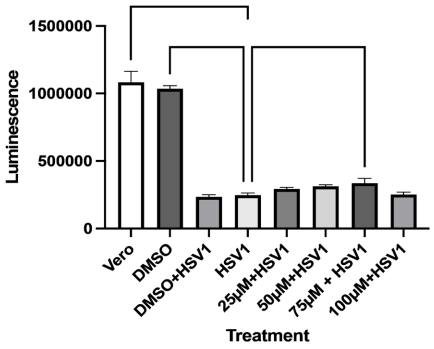

(C) Post-penetration

Figure 6. (A) ToxGlo™ attachment assay of Vero cells infected at 4˚C with HISP-1 treated HSV-1, pretreated for 1 h with 25 - 100 μM concentrations of HISP-1 and Vero cells infected with untreated HISP-1 as a control. The antiviral effects of HISP-1 on the attachment stage of HSV-1 infection are reported. Cell viability was measured by the luminescence of Vero cells. (B) ToxGlo penetration assay of Vero cells infected at 4˚C for 2 h to ensure attachment but not penetration of the virions. The cells were treated for 10 min at varying concentrations of HISP-1 at room temperature during the penetration step [35] of infection. After 48 h, cell viability as measured by the luminescence of Vero cells infected with 25 - 100 μM concentrations of HISP-1-treated HSV-1 and Vero cells infected with untreated HISP-1 as a control. The antiviral effects of HISP-1 on the penetration stage of HSV-1 infection are reported. Cell viability was measured by the luminescence of Vero cells infected with 25 - 100 μM concentrations of HISP-1-treated HSV-1 and Vero cells infected with untreated HISP-1 as a control. **p<0.01, ***p < 0.001, ****p < 0.0001.

3.4. Fluorescent Microscopy Indicates that Treatment of HSV-1 with HISP-1 Inhibits the Infection of Vero Cells

The strain of HSV-1 used in this study, HSV-1 GHSV-UL46, contains the sequence for GFP fused to the tegument protein pUL46. GFP expression (green) occurs in a late stage of HSV-1 infection. DAPI stain (blue) shows the morphology of the cell nuclei. GFP expression is greatest when untreated HSV-1 infected Vero cells (B). HSV-1 infected cells show cytopathic effects characteristic of morphologic changes shown in human herpes virus infections including cytoskeletal modifications resulting in the appearance of elongated cells and formation of multinucleated cells [36]. There is a difference in GFP expression and morphology between in the untreated and treated HSV-1 infected Vero cells at 12 hpi. Expression of GFP is inhibited in HSV-1 infected cells when virions were treated with 75 μM HISP-1 (**Figure 7**).

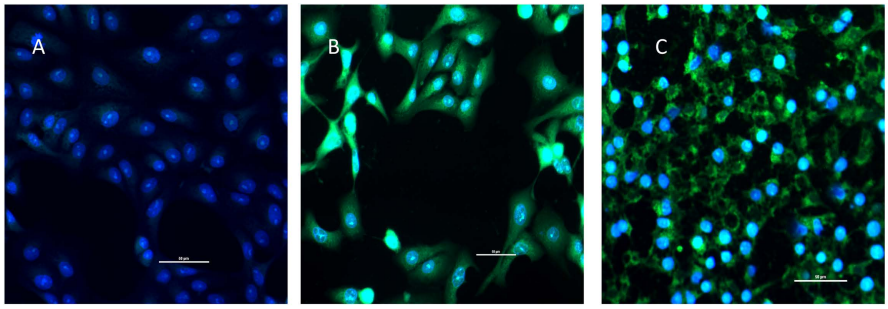

Figure 7. Fluorescent microscopic images (200×) of (A) uninfected Vero cells; (B) 12 h post-infection observation of untreated HSV-1 infected Vero cells and (C) HISP-1 treated HSV-1 infected Vero cells (Scale = 50 μM).

3.5. Molecular Docking Analyses Indicated That HISP-1 Has Low Binding Affinity to gD

Molecular docking analyses were conducted to model the interaction between the receptor-binding protein gD and HISP-1. The predicted interactions between gD and HISP-1 and curcumin were also analyzed because of the structural similarities between hispolons and curcumin. The 3D structures for HISP-1 and curcumin are presented in **Figures 8(A)** and **Figures 8(B)**. The predicted ribbon model of the binding of HISP-1 to gD is shown in **Figures 8(C)**. HISP-1 forms five conventional hydrogen bonds (Chain A: two with VAL 61 and Chain B: 115 TYR, 131 THR, and 132 GLN) and four pi-alkyl bonds (Chain A: 60 ALA; Chain B: 115 TYR, 130 ARG, and 133 PRO (**Figures 8(E)**). HISP-1 failed to meet the -7 kcal/mol threshold with a reported receptor binding affinity of −6.15 kcal/mol.

Analysis with AutoDock Vina showed that curcumin can bind to gD with a binding affinity of −7.17 kcal/mol. Predicted binding interactions between curcumin and gD are shown in **Figure 8(D)**, with a summary of receptor ligand interactions in **Figure 8(F)**. Based on these analyses, curcumin forms three conventional hydrogen bonds (Chain B: 130 ARG, 133 PRO, 222 ARG), five alkyl/pi-alkyl bonds (Chain B: 113 MET, 130 ARG, two with 133 PRO, 222

ARG), and van der Waals interactions with nine residues (Chain A: 70 LEU, 72 HIS; Chain B: 115 TYR, 131 THR, 132 GLN, 134 ARG, 135 TRP, 148 ASN, 221 PRO).

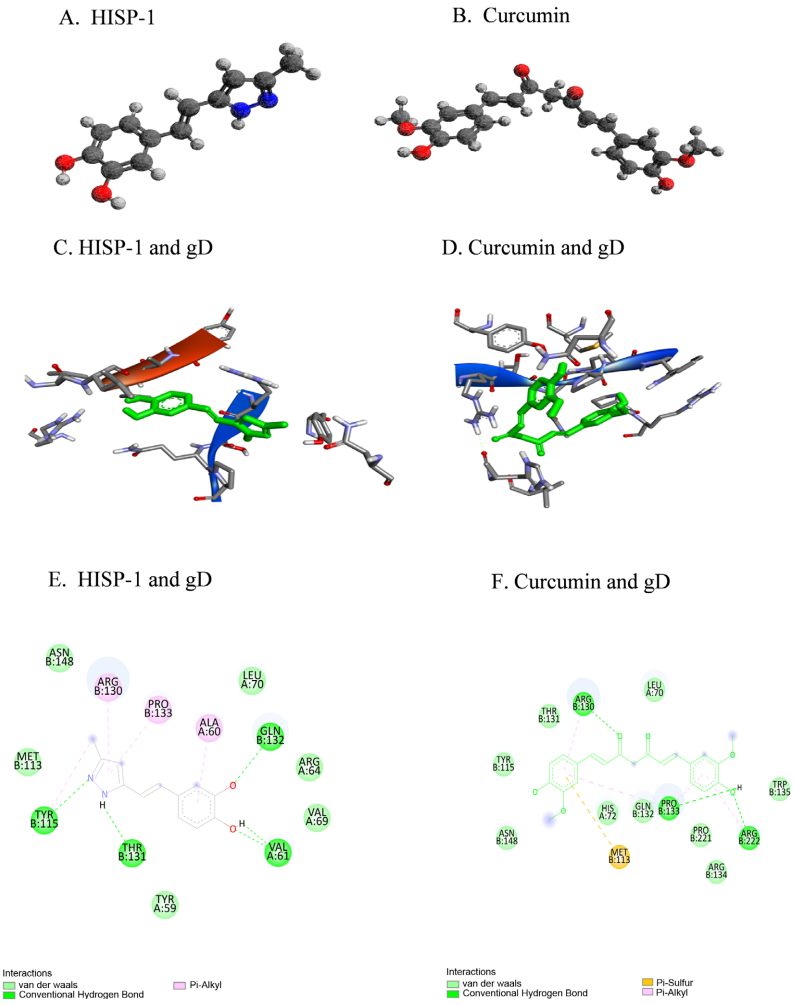

Figure 8. Molecular docking analysis of the interaction of HSV-1 (gD) and HISP-1 and curcumin. 3D structure of HISP-1 (A) and curcumin (B). Ribbon model of predicted binding interaction between HISP-1 and gD (C) an HISP-1 and curcumin (D); (E) Two-dimensional diagram of receptor-ligand interactions between HISP-1 and gD and (F) curcumin and gD, including conventional hydrogen bonds (green), van der Waals interactions (light green) and pi-alkyl (pink).

4. Discussion

There has been extensive research on the medicinal properties and modes of action of hispolon, a polyphenolic constituent of medicinal mushrooms and hispolon analogs. Medicinal properties include antioxidant, anti-inflammatory, and antiproliferative [1] [2] [3] [4] [23] [36] [37] There is, however, a paucity of research on the antiviral properties. Curcumin, structurally similar to hispolon, has also demonstrated antioxidant [6], anti-inflammatory [7] [8], antibacterial [9], and antiviral activities against hepatitis C virus [10], enterovirus 71 [11],

human immunodeficiency virus [12], influenza A [13], and herpes simplex virus (HSV) 1 and 2 [14] [15]. Curcumin acts as an antiviral through multiple mechanisms [17]. The structural similarities to curcumin suggest a role of hispolon as an antiviral.

In this study we investigated the ability of 24 hispolon analogs to inhibit the infection of HSV-1 in cultured Vero cells. Of the 24 analogues tested only hispolon pyrazole-1 (HISP-1) inhibited the infection of Vero cells by HSV-1 (**Table 1**, **Figure 3-5**). HISP-1 has therapeutic potential; our results indicate that it can be safely applied to cultured Vero cells at concentrations up to 125 μM (**Figure 1**). The early stages of HSV-1 infection are affected by treatment of the virions with HISP-1 (**Figure 6(A)-(C)**). The expression of the structural proteins (tegument and surface glycoproteins) is also inhibited when the virus is treated with HISP-1. There is a reduction in the expression of GFP (sequence bound to the tegument protein) following treatment with HISP-1.

HSV-1 infections continue to affect a large population of the world's population [19]. HSV-1 causes cold sores around the mouth and oral and lesions in the genital mucosa [38]. HSV-1 also causes severe illness such as encephalitis [39], necrotizing stromal keratitis [40], and neonatal herpes [41]. There are effective medications for the treatment of HSV-1 such as acyclovir, which acts on the HSV polymerase thymidine kinase [42]. Prolonged use of acyclovir can lead to resistance because of mutations in the thymidine kinase gene and possibility the development of ACV resistant strains [43] [44]. Viral transmission occurs by direct contact with lesions or infected secretions [45]. HSV-1 infection requires high affinity binding of cellular receptors to gD [46]. Cellular receptors such as herpes virus entry mediator (HVEM), nectin-1, and 3-O-sulfated heparan sulfate then interact with gD, inducing a conformational change that leads to formation of a fusion complex composed of several viral glycoproteins (gB, gH, and gL). The viral nucleocapsid and tegument are then released into the cytoplasm [46] [47]. Results of this investigation indicate that HISP-1 affects early stages of viral infection: attachment, penetration, and post-penetration (**Figure 6(A)**, **Figure 6(B)**, and **Figure 6(C)**, respectively). This mechanism of inhibition is similar to the effect of curcumin on the attachment and penetration of HSV-1 [14] but differs in that HISP-1 also demonstrated an effect post-penetration (**Figure 6(C)**). However, curcumin reported greater antiviral cell viability and inhibitory abilities against HSV-1 in cultured Vero cells [14] than our results with HISP-1 in this study.

One interesting aspect of the results that compared the antiviral effect of treatment of the cells to treatment of the virus is that treatment of the cells with HISP-1 did not significantly inhibit HSV-1 infection (**Figure 4(B)** and **Figure 5(B)**). Antiviral therapeutics often target the viral attachment protein required for infection or the immune system [48]. Our results imply that HISP-1 targets the surface glycoproteins.

Molecular docking analyses were conducted to model the interaction between

the receptor-binding protein gD and HISP-1 and between gD and curcumin (**Figure 8**). Computational docking has been used to identify potential natural inhibitors of the receptor-binding domain of SARS-CoV-2 based on number of hydrogen bonds, and binding affinity minimum interaction energy [48]. The binding affinities of HISP-1 to gD and curcumin to gD were −6.15 kcal/mole and −7.15 kcal/mole, respectively. The binding affinity of HISP-1 to gD is lower than the desired −7.0 kcal/mole threshold. This finding alone does not preclude consideration of HISP-1 as an antiviral against HSV-1. The binding affinity of some Food and Drug Administration (FDA) approved drugs against HIV-1 reverse transcriptase ranged from −5.63 to −6.85 [49]. It is possible that HISP-1, like curcumin, exerts antiviral effects through multiple mechanisms, including maintaining the infected cell's redox balance [50]. Future studies should investigate the effect of HISP-1 on expression of non-structural proteins and on alleviating oxidative stress. Additionally, in vivo studies should be conducted to determine the effectiveness of HISP-1 in inhibiting HSV-1 infection in an animal model.

5. Conclusion

Our results demonstrate that HISP-1 is safe at concentrations tested and a concentration of 75 μM showed a maximum cell viability and inhibition of 78% and 62.7%, respectively. HISP-1 acts on the early stages of HSV-1 infection. HISP-1 could work in synergy with other antivirals that work by a different modality and could be developed as a component of a topical agent to reduce the spread of HSV-1.

Acknowledgements

We thank Kelli A. Duncan for graphical and statistical analyses.

Author Contributions

Conceptualization, G.V.S., M.V.R. and S.D.A.; methodology, S.D.A. and K.T.B..; formal analysis, S.D.A. and K.T.B investigation, S.D.A. and K.T.B.; resources, G.V.S., M.V.R. and S.D.A.; writing—original draft preparation, S.D.A and K.T.B; writing—review and editing, S.D.A., K.T.B, G.V.S., and M.V.R. All authors have read and agreed to the published version of the manuscript.

Funding

This research was funded in part by the Faculty Scholarship Program, Montclair State University.

Conflicts of Interest

The authors declare no conflicts of interest regarding the publication of this paper.

References

[1] Yang, L.Y., Shen, S.C., Cheng, K.T., Subbaraju, G.V., Chien, C.C. and Chen, Y.C. (2014) Hispolon Inhibition of Inflammatory Apoptosis through Reduction of iN-

OS/NO Production *via* HO-1 Induction in Macrophages. *Journal of Ethnopharmacology*, **156**, 61-72. https://doi.org/10.1016/j.jep.2014.07.054

[2] Venkateswarlu, S., Ramachandra, M., Sethuramu, K. and Subbaraju, G.V. (2002) Synthesis and Antioxidant Activity of Hispolon, a Yellow Pigment from *Inonotus hispidius*. *Indian Journal of Chemistry*, **41**, 875-877.

[3] Ali, N.A., Jansen, R., Pilgrim, H., Liberra, K. and Lindequist, U. (1996) Hispolon, a Yellow Pigment from *Inonotus hispidus*. *Phytochemistry*, **41**, 927-929. https://doi.org/10.1016/0031-9422(95)00717-2

[4] Fan, H.C., Hsieh, Y.C., Li, L.H., Chang, C.C., Janoušková, K., Ramani, M.V., Subbaraju, G.V., Cheng, K.T. and Chang, C.C. (2020) Dehydroxyhispolon Methyl Ether, A Hispolon Derivative, Inhibits WNT/β-Catenin Signaling to Elicit Human Colorectal Carcinoma Cell Apoptosis. *International Journal of Molecular Sciences*, **21**, Article 8839. https://doi.org/10.3390/ijms21228839

[5] Awadh Ali, N.A., Mothana, R.A., Lesnau, A., Pilgrim, H. and Lindequist, U. (2003) Antiviral Activity of *Inonotus hispidus*. *Fitoterapia*, **74**, 483-485. https://doi.org/10.1016/S0367-326X(03)00119-9

[6] Jakubczyk, K., Drużga, A., Katarzyna, J. and Skonieczna-Żydecka, K. (2020) Antioxidant Potential of Curcumin—A Meta-Analysis of Randomized Clinical Trials. *Antioxidants*, **9**, Article 1092. https://doi.org/10.3390/antiox9111092

[7] Menon, V.P. and Sudheer, A.R. (2007) Antioxidant and Anti-Inflammatory Properties of Curcumin. *Advances in Experimental Medicine and Biology*, **595**, 105-125. https://doi.org/10.1007/978-0-387-46401-5_3

[8] He, Y., Yue Y., Zheng, X., Zhang, K., Chen, S. and Du, Z. (2015) Curcumin, Inflammation, and Chronic Diseases: How Are They Linked? *Molecules*, **20**, 9183-9213. https://doi.org/10.3390/molecules20059183

[9] Qu, L., Li, X., Zhou, J., Cao, K., Xie, Q., Zhou, P., Qian, W. and Yang, Y. (2023) A Novel Dual-Functional Coating Based on Curcumin/APEG Polymer with Antibacterial and Antifouling Properties. *Applied Surface Science*, **627**, Article ID: 157224. https://doi.org/10.1016/j.apsusc.2023.157224

[10] Yusuf, H., Novitasari, E.K.D.D., Purnami, N.L.W., Mahbub, A.W., Sari, R. and Setyawan, D. (2022) Formulation Design and Cell Cytotoxicity of Curcumin-Loaded Liposomal Solid Gels for Anti-Hepatitis C Virus. *Advances in Pharmacological and Pharmaceutical Sciences*, **2022**, Article ID: 3336837. https://doi.org/10.1155/2022/3336837

[11] Qin, Y., Lin, L., Chen, Y., Wu, S., Si, X., Wu, H., Zhai, X., Wang, Y., Tong, L., Pan, B., Zhong, X., Wang, T., Zhao, W. and Zhong, Z. (2014) Curcumin Inhibits the Replication of Enterovirus 71 *in Vitro*. *Acta Pharmaceutica Sinica B*, **4**, 284-294. https://doi.org/10.1016/j.apsb.2014.06.006

[12] Guo, L., Xing, Y., Pan, R., Jiang, M., Gong, Z., Lin, L., Wang, J., Xiong, G. and Dong, J. (2013) Curcumin Protects Microglia and Primary Rat Cortical Neurons against HIV-1 gp120-Mediated Inflammation and Apoptosis. *PLOS ONE*, **8**, e70565. https://doi.org/10.1371/journal.pone.0070565

[13] Dai, J., Gu, L., Su,Y., Wang, Q., Zhao, Y., Chen, X., Deng, H., Li, W., Wang, G. and Li, K. (2018) Inhibition of Curcumin on Influenza A Virus Infection and Influenzal Pneumonia *via* Oxidative Stress, TLR2/4, p38/JNK MAPK and NF-κB Pathways. *International Immunopharmacology*, **54**, 177-187. https://doi.org/10.1016/j.intimp.2017.11.009

[14] Flores, D.J., Lee, L.H. and Adams, S.D. (2016) Inhibition of Curcumin-Treated Herpes Simplex Virus 1 and 2 in Vero Cells. *Advances in Microbiology*, **6**, 276-287.

https://doi.org/10.4236/aim.2016.64027

[15] Vitali, D., Bagri, P., Wessels, J.M., Arora, M., Ganugula, R., Parikh, A., Mandur, T., Felker, A., Garg, S., Kumar, M.N.V.R. and Kaushic, C. (2020) Curcumin Can Decrease Tissue Inflammation and the Severity of HSV-2 Infection in the Female Reproductive Mucosa. *International Journal of Molecular Sciences*, **21**, Article 337. https://doi.org/10.3390/ijms21010337

[16] Priyadarsini, K.I. (2014) The Chemistry of Curcumin: From Extraction to Therapeutic Agent. *Molecules*, **19**, 20091-20112. https://doi.org/10.3390/molecules191220091

[17] Šudomová, M. and Hassan, S.T.S. (2021) Nutraceutical Curcumin with Promising Protection against Herpesvirus Infections and Their Associated Inflammation: Mechanisms and Pathways. *Microorganisms*, **9**, Article 292. https://doi.org/10.3390/microorganisms9020292

[18] Abd El-Halim, S.M., Mamdouh, M.A., El-Haddad, A.E. and Soliman, S.M. (2020) Fabrication of Anti-HSV-1 Curcumin Stabilized Nanostructured Proniosomal Gel: Molecular Docking Studies on Thymidine Kinase Proteins. *Scientia Pharmaceutica*, **88**, Article 9. https://doi.org/10.3390/scipharm88010009

[19] WHO (2023) Herpes Simplex Virus. https://www.who.int/news-room/fact-sheets/detail/herpes-simplex-virus

[20] Spear, P.G., Manoj, S., Yoon, M., Jogger, C.R., Zago, A. and Myscofski, D. (2006) Different Receptors Binding to Distinct Interfaces on Herpes Simplex Virus gD Can Trigger Events Leading to Cell Fusion and Viral Entry. *Virology*, **344**, 17-24. https://doi.org/10.1016/j.virol.2005.09.016

[21] Fan, Q., Kopp, S.J., Connolly, S.A. and Longnecker, R. (2017) Structure-Based Mutations in the Herpes Simplex Virus 1 Glycoprotein B Ectodomain Arm Impart a Slow-Entry Phenotype. *mBio*, **8**, e00614-17. https://doi.org/10.1128/mBio.00614-17

[22] Lei, Y., Chen, W., Liang, H., Wang, Z., Chen, J., Hong, H., Xie, L., Nie, H. and Xiong, S. (2019) Preparation of a MonoPEGylated Derivative of Cyanovirin-N and Its Virucidal Effect on Acyclovir-Resistant Strains of Herpes Simplex Virus Type 1. *Archives of Virology*, **164**, 1259-1269. https://doi.org/10.1007/s00705-018-04118-4

[23] Balaji, N.V., Ramani, M.V., Viana, A.G., Sanglard, L.P., White, J., Mulabagal, V., Lee, C., Gana, T.J., Egiebor, N.O., Subbaraju, G.V. and Tiwari, A.K. (2015) Design, Synthesis and *in Vitro* Cell-Based Evaluation of the Anti-Cancer Activities of Hispolon Analogs. *Bioorganic & Medicinal Chemistry*, **23**, 2148-2158. https://doi.org/10.1016/j.bmc.2015.03.002

[24] Ravindran, J., Subbaraju, G.V., Ramani, M.V., Sung, B. and Aggarwal, B.B. (2010) Bisdemethylcurcumin and Structurally Related Hispolon Analogues of Curcumin Exhibit Enhanced Prooxidant, Anti-Proliferative and Anti-Inflammatory Activities *in Vitro*. *Biochemical Pharmacology*, **79**, 1658-1666. https://doi.org/10.1016/j.bcp.2010.01.033

[25] Balaji, N.V., HariBabu, B., Rao, V.U., Subbaraju, G.V., Nagasree, K.P. and Kumar, M.M.K. (2019) Synthesis, Screening and Docking Analysis of Hispolon Pyrazoles and Isoxazoles as Potential Antitubercular Agents. *Current Topics in Medicinal Chemistry*, **19**, 662-682. https://doi.org/10.2174/1568026619666190305124954

[26] Rossi, M., Caruso, F., Costanzini, I., Kloer, C., Sulovari, A., Monti, E., Gariboldi, M., Marras, E., Balaji, N.V., Ramani, M.V. and Subbaraju, G.V. (2019) X-Ray Crystal Structures, Density Functional Theory and Docking on Deacetylase Enzyme for Antiproliferative Activity of Hispolon Derivatives on HCT116 Colon Cancer. *Bioorganic & Medicinal Chemistry*, **27**, 3805-3812.

https://doi.org/10.1016/j.bmc.2019.07.008

[27] Willard, M. (2002) Rapid Directional Translocations in Virus Replication. *Journal of Virology*, **76**, 5220-5232. https://doi.org/10.1128/JVI.76.10.5220-5232.2002

[28] Pettersen, E.F., Goddard, T.D., Huang, C.C., Couch, G.S., Greenblatt, D.M., Meng, E.C. and Ferrin, T.E. (2004) UCSF Chimera—A Visualization System for Exploratory Research and Analysis. *Journal of Computational Chemistry*, **25**, 1605-1612. https://doi.org/10.1002/jcc.20084

[29] Morris, G.M., Huey, R., Lindstrom, W., Sanner, M.F., Belew, R.K., Goodsell, D.S. and Olson, A.J. (2009) Autodock4 and AutoDockTools4: Automated Docking with Selective Receptor Flexibility. *Journal of Computational Chemistry*, **16**, 2785-2791. https://doi.org/10.1002/jcc.21256

[30] Tian, W., Chen, C., Lei, X., Zhao, J. and Liang, J. (2018) CASTp 3.0: Computed Atlas of Surface Topography of Proteins. *Nucleic Acids Research*, **46**, W363-W367. https://doi.org/10.1093/nar/gky473

[31] Hanwell, M.D., Curtis, D.E., Lonie, D.C. Vandermeersch, T., Zurek, E. and Hutchison, G.R. (2012) Avogadro: An Advanced Semantic Chemical Editor, Visualization, and Analysis Platform. *Journal of Cheminformatics*, **4**, Article No. 17. https://doi.org/10.1186/1758-2946-4-17

[32] Eberhardt, J., Santos-Martins, D., Tillack, A.F. and Forli, S. (2021) AutoDock Vina 1.2.0: New Docking Methods, Expanded Force Field, and Python Bindings. *Journal of Chemical Information and Modeling*, **61**, 3891-3898. https://doi.org/10.1021/acs.jcim.1c00203

[33] Trott, O. and Olson, A.J. (2010) AutoDock Vina: Improving the Speed and Accuracy of Docking with a New Scoring Function, Efficient Optimization, and Multithreading. *Journal of Computational Chemistry*, **31**, 455-461. https://doi.org/10.1002/jcc.21334

[34] Aguilar, J.S., Roy, D., Ghazal, P. and Wagner, E.K. (2002) Dimethyl Sulfoxide Blocks Herpes Simplex Virus-1 Productive Infection *in Vitro* Acting at Different Stages with Positive Cooperativity. Application of Micro-Array Analysis. *BMC Infectious Diseases*, **2**, Article No. 9. https://doi.org/10.1186/1471-2334-2-9

[35] Harden, E.A., Falshaw, R., Carnachan, S.M., Kern, E.R. and Prichard, M.N. (2009) Virucidal Activity of Polysaccharide Extracts from Four Algal Species against Herpes Simplex Virus. *Antiviral Research*, **83**, 282-289. https://doi.org/10.1016/j.antiviral.2009.06.007

[36] Chethna, P., Iyer, S.S., Gandhi, V.V., Kunwar, A., Singh, B.G., Barik, A., Balaji, N.V., Ramani, M.V., Subbaraju, G.V. and Priyadarsini, K.I. (2018) Toxicity and Antigenotoxic Effect of Hispolon Derivatives: Role of Structure in Modulating Cellular Redox State and Thioredoxin Reductase. *ACS Omega*, **3**, 5958-5970. https://doi.org/10.1021/acsomega.8b00415

[37] Sarfraz, A., Rasul, A., Sarfraz, I., Shah, M.A., Hussain, G., Shafiq, N., Masood, M., Adem, Ş., Sarker, S.D. and Li, X. (2020) Hispolon: A Natural Polyphenol and Emerging Cancer Killer by Multiple Cellular Signaling Pathways. *Environmental Research*, **190**, Article ID: 110017. https://doi.org/10.1016/j.envres.2020.110017

[38] Ryder, N., Jin, F., McNulty, A.M., Grulich, A.E. and Donovan, B. (2009) Increasing Role of Herpes Simplex Virus Type 1 in First-Episode Anogenital Herpes in Heterosexual Women and Younger Men Who Have Sex with Men, 1992-2006. *Sexually Transmitted Infections*, **85**, 416-419. https://doi.org/10.1136/sti.2008.033902

[39] Bradshaw, M.J. and Venkatesan, A. (2016) Herpes Simplex Virus-1 Encephalitis in Adults: Pathophysiology, Diagnosis, and Management. *Neurotherapeutics*, **13**, 493-

508. https://doi.org/10.1007/s13311-016-0433-7

[40] Azher, T.N., Yin, X.T., Tajfirouz, D., Huang, A.J. and Stuart, P.M. (2017) Herpes Simplex Keratitis: Challenges in Diagnosis and Clinical Management. *Clinical Ophthalmology*, **11**, 185-191. https://doi.org/10.2147/OPTH.S80475

[41] Belshe, R.B., Leone, P.A., Bernstein, D.I., Wald, A., Levin, M.J., Stapleton, J.T., Gorfinkel, I., Morrow, R.L.A., Ewell, M.G., Stokes-Riner, A., Dubin, G., Heineman, T.C., Schulte, J.M. and Deal, C.D. (2012). Efficacy Results of a Trial of a Herpes Simplex Vaccine. *The New England Journal of Medicine*, **366**, 34-43. https://doi.org/10.1056/NEJMoa1103151

[42] Elion, G.B. (1993) Acyclovir: Discovery, Mechanism of Action and Selectivity. *Journal of Medical Virology*, **41**, 2-6. *https://doi.org/10.1002/jmv.1890410503*

[43] Frobert, E., Cortay, J.C., Ooka, T., Najioullah, F., Thouvenot, D., Lina, B. and Morfin, F. (2008) Genotypic Detection of Acyclovir-Resistant HSV-1: Characterization of 67 ACV-Sensitive and 14 ACV-Resistant Viruses. *Antiviral Research*, **79**, 28-36. https://doi.org/10.1016/j.antiviral.2008.01.153

[44] Sergerie, Y. and Boivin, G. (2006) Thymidine Kinase Mutations Conferring Acyclovir Resistance in Herpes Simplex Type 1 Recombinant Viruses. *Antimicrob. Antimicrobial Agents and Chemotherapy*, **50**, 3889-3892. https://doi.org/10.1128/AAC.00889-06

[45] Ramchandani, M., Kong, M., Tronstein, E., Selke, S., Mikhaylova, A., Magaret, A., Huang, M.L., Johnston, C., Corey, L. and Wald, A. (2016) Herpes Simplex Virus Type 1 Shedding in Tears and Nasal and Oral Mucosa of Healthy Adults. *Sexually Transmitted Diseases*, **43**, 756-760. https://doi.org/10.1097/OLQ.0000000000000522

[46] Clarke, R.W. (2015) Forces and Structures of the Herpes Simplex Virus (HSV) Entry Mechanism. *ACS Infect. Dis*, **1**, 403-415. https://doi.org/10.1021/acsinfecdis.5b00059

[47] Subramanian, R.P. and Geraghty, R.J. (2007) Herpes Simplex Virus Type 1 Mediates Fusion through a Hemifusion Intermediate by Sequential Activity of Glycoproteins D, H, L, and B. *Proceedings of the National Academy of Sciences of the United States of America*, **104**, 2903-2908. https://doi.org/10.1073/pnas.0608374104

[48] Mathew, S.M., Benslimane, F., Althani, A.A. and Yassine, H.M. (2021) Identification of Potential Natural Inhibitors of the Receptor-Binding Domain of the SARS-CoV-2 Spike Protein Using a Computational Docking Approach. *Qatar Medical Journal*, **2021**, Article 12. https://doi.org/10.5339/qmj.2021.12

[49] Terefe, E.M. and Ghosh, A. (2022) Molecular Docking, Validation, Dynamics Simulations, and Pharmacokinetic Prediction of Phytochemicals Isolated from *Croton dichogamus* against the HIV-1 Reverse Transcriptase. *Bioinform Biol Insights.* **16**. https://doi.org/10.1177/11779322221125605

[50] Rahban, M., Habibi-Rezaei, M., Mazaheri, M., Saso, L. and Moosavi-Movahedi, A.A. (2020) Anti-Viral Potential and Modulation of Nrf2 by Curcumin: Pharmacological Implications. *Antioxidants*, **9**, Article 1228. https://doi.org/10.3390/antiox9121228